HHS Public Access

Author manuscript

Nat Chem Biol. Author manuscript; available in PMC 2013 June 01.

Published in final edited form as:

Nat Chem Biol. 2012 December ; 8(12): 975–981. doi:10.1038/nchembio.1092.

The unanticipated complexity of the selectivity-filter glutamates of nicotinic receptors

Gisela D. Cymes[1] and **Claudio Grosman**[1,*]

[1]Department of Molecular and Integrative Physiology, Center for Biophysics and Computational Biology, and Neuroscience Program, University of Illinois at Urbana-Champaign, Urbana, IL 61801, USA

Abstract

In ion channels, “rings” of ionized side chains that decorate the walls of the permeation pathway often lower the energetic barrier to ion conduction. Using single-channel electrophysiological recordings, we studied the poorly understood ring of four glutamates (and one glutamine) that dominate this catalytic effect in the muscle nicotinic acetylcholine receptor (“the intermediate ring of charge”). We show that all four wild-type glutamate side chains are deprotonated in the 6.0–9.0 pH range; that only two of them contribute to the size of the single-channel current; that these side chains must be able to adopt alternate conformations that either allow or prevent their negative charges from increasing the rate of cation conduction; and that the location of these glutamate side chains squarely at one of the ends of the transmembrane pore is critical for their largely unshifted pK_a values and for the unanticipated impact of their conformational flexibility on cation permeation.

It has long been appreciated that the ring of glutamates at the intracellular end of the transmembrane pore (the “intermediate ring”) is one of the main determinants of ion-conduction properties in the cation-selective nicotinic acetylcholine receptors[1] (AChRs). Although having little effect on the cation-*versus*-anion selectivity of these channels (as probed with glutamate-to-alanine mutations[2–4]), the effect of this ring on the size (or “amplitude”) of the single-channel current is larger than the effect of any of the other naturally-occurring rings of pore-lining acidic side chains[1]. Because mutations at adjacent positions (involving non-ionizable residues) do render the AChR anion selective[2,4], the region as a whole is typically referred to as the “charge-selectivity filter”. Other cation-selective channels, such as the (four-domain) voltage-dependent Ca^{2+} (Ca_V) channels and the (tetrameric) cyclic-nucleotide gated (CNG) channels, also contain rings of acidic side chains in their selectivity-filter regions, but the functional properties of these rings differ markedly from those of the AChR. One of the most intriguing differences is the interaction

Correspondence should be addressed to C.G. 407 S. Goodwin Ave., 524 Burrill Hall, Urbana, IL 61801. grosman@illinois.edu.

Author Contributions G.D.C. and C.G. designed experiments, analyzed data and wrote the manuscript; G.D.C performed experiments.

Competing Financial Interests The authors declare no competing financial interests.

of these rings of carboxylates with protons: whereas the protonation state of the glutamate side chains of Ca_V and CNG channels is sensitive to pH changes in the 6.0–9.0 range (as evidenced by the stepwise decrease in single-channel current amplitude as the proton concentration is increased[5–7]), the protonation state of the glutamates in the intermediate ring of the AChR is not. Because elucidating the basis of these differences may shed light into the mechanisms underlying the widely different Ca^{2+}-conducting parameters of these channels, we set out to unravel the properties of these glutamates in the AChR. Indeed, for example, while extracellular Ca^{2+} reduces inward currents carried by ~150 mM Na^+ with an apparent affinity of ~1 μM in the case of L-type Ca_V channels of ventricular heart cells[8], this value is ~5–10 mM for the muscle AChR[9], and while the single-channel conductance in the presence of ~100–150 mM extracellular Ca^{2+} as the main permeant cation is ~9 pS for the L-type channels[8], that for the muscle AChR is ~30 pS; ref. 9.

Overall, our analysis of the effect of mutations, pH changes, and H_2O-to-D_2O solvent substitution on the AChR's single-channel current properties revealed that the intermediate ring of acidic side chains form a system of much higher complexity than could be anticipated from this channel's extremely simple conductance behavior. Certainly, not only the protonation state, but also, the location along the long axis of the pore and the conformation of these side chains seem to be key determinants of the cation-conduction free-energy profile.

RESULTS

Not all four glutamates contribute to cation conduction

The adult muscle AChR is a heteropentameric complex of two α1 subunits and one each of β1, δ and ε subunits. The intermediate ring of glutamates of the wild-type channel consists of four glutamates and one glutamine, and its position along the amino-acid sequence is usually referred to as position –1′ (for an introduction to the muscle AChR and the effect of the glutamates at position –1′ on charge selectivity and single-channel current size, see Supplementary Results, Supplementary Figs. 1 and 2).

To increase the mean duration of bursts of single-channel openings, and thus to allow a careful analysis of the open-channel current signal, we engineered a gain-of-function mutation in the background of most of the muscle AChR constructs studied here (details are given in the figure legends). Using this approach, we found that, in the nominal absence of extracellular divalent cations and with ~150 mM K^+ as the main permeant cation, the single-channel current–voltage (*i*–*V*) relationship recorded from the mutant containing a full ring of alanines at position –1′ displays a marked inward rectification and a conductance (in the inward direction) of ~30 pS (Fig. 1a). At −100 mV, for example, the single-channel current through this mutant (~1.8 pA) is lower than that through the wild-type AChR (~13.5 pA) by a factor of ~7.5. The presence of a single glutamate (in any of the four types of subunit) increases the conductance by ~50 pS, whereas the presence of two glutamates (in the β1 and δ subunits) increases the conductance by ~100 pS and partly relieves the rectification (Fig. 1a). The value of ~140 pS found for the AChR containing only two glutamates in the intermediate ring was quite unexpected because the wild-type's single-channel conductance under the same ion conditions is, also, ~140 pS. To learn whether a value of ~140 pS

represents a “ceiling” beyond which the conductance cannot increase, we recorded single-channel activity from a mutant containing a full ring of five glutamates. We found the conductance of this mutant to be ~185 pS (Fig. 1a), consistent with the notion of a ~30-pS “baseline” and three steps of ~50 pS. From these results we infer that, in the wild-type AChR, only two of the four glutamates contribute to the cation-conduction rate, and that each of these contributes a ~50 pS increment. Similarly, in the mutants containing a full ring of glutamates (and thus resembling the non-muscle AChRs), only three of the five glutamates contribute to set the size of the unitary current. So, what happens to the other two glutamates? Are they permanently protonated? Evidently, the notion that each glutamate in the intermediate ring bears a negative charge and that each negative charge makes a similar contribution to the size of the single-channel current (an idea that has prevailed since the early work of ref. 1) was in need of revision.

The ε-subunit glutamine provides mechanistic insight

The observation that the single-channel conductance of the wild-type channel cannot be “titrated” in a step-wise fashion in the 6.0–9.0 pH range (Fig. 1b) led us to speculate that, perhaps, the pK_a values of two of the wild-type glutamates are $\ll$ 6.0, whereas the pK_a values of the other two glutamates are $\gg$ 9.0. pK_a shifts of this sort occur whenever carboxylates are close enough to one another so as to form hydrogen bonds and/or interact electrostatically[10–13] and would certainly explain the observed pH insensitivity. However, other mechanisms could not be ruled out.

While testing the effect of several mutations at position –1′ (Fig. 2), we noted that the open-channel current of the mutant containing a glutamine in the ε subunit, two alanines in both α1 subunits and two glutamates in β1 and δ fluctuates between two discrete levels (henceforth, we will refer to this mutant as the “AQAEE” AChR in reference to the side chains occupying the intermediate ring in the α1, ε, α1, β1 and δ subunits, respectively; according to this naming system, the wild-type channel is “EQEEE”; see Supplementary Fig. 1b). The conductance of the high-conductance level is ~132 pS, that is, very close to the ~140-pS value of the AAAEE construct. The conductance of the sublevel, on the other hand, is ~85 pS and displays a marked inward rectification, two properties that are highly reminiscent of the conductance behavior of the mutants containing a single glutamate (and four alanines) in the –1′ ring. In addition, we found that, although the presence of alanines in the α1 subunits is not required for this phenomenon to be observed, the presence of a glutamine in ε apparently is (compare Fig. 2a, b). Because glutamine is the naturally-occurring amino acid at this position of the ε subunit, we decided to pay close attention to these main-level $\leftrightharpoons$ sublevel interconversions in hopes that understanding this remarkable phenomenon would help us tease out the complexity of the wild-type ring of glutamates. Because the mutant bearing a glutamine in the α1 subunit (the QQQEE mutant) seemed to be the one giving rise to the most robust channel activity, we used this variant for the more demanding experiments.

To determine whether the observed open-channel current fluctuations are the electrical manifestation of the alternate protonation and deprotonation of one of the two glutamates at position –1′ (see refs. 14, 15), outside-out patches were symmetrically bathed by solutions of

pH ranging from 6.0 to 8.5. Single-channel recordings from the QQQEE channel revealed only a weak effect of proton concentration on the relative occupancies of the two open-channel current levels (Fig. 3a), much weaker than that observed for AChRs engineered to bear single glutamates at other pore-lining positions along the M2 α-helical transmembrane segments (Fig. 3b; see also Supplementary Figs. 1a and 2a). Because the protonation–deprotonation of nearby ionizable side chains may well mask the pH dependence of the protonation state of the glutamates at position –1′ (as is often the case for proteins containing clusters of electrostatically interacting ionizable side chains[16–21]; Supplementary Fig. 3), we replaced the four aspartates at position –5′ with alanines and quantified the effect of symmetrical pH changes on the conductance behavior of this multiple mutant. Again, we found that the effect of pH is uncharacteristically weak (Fig. 3c), as if the subconductance level were not the result of proton binding to an ionizable side chain. To further challenge this notion, we tested the effect of replacing the labile protium atoms with deuterium by changing the solvent from H_2O to D_2O. If the observed high $\leftrightharpoons$ low conductance-level fluctuations resulted from an acid–base reaction, then both the forward and reverse rates would be expected to become slower upon protium-to-deuterium substitution because of the known effect of isotopic substitution on the zero-point vibrational energies of the ground states and transition state of acid–base equilibria[22]. First, as a control, we measured the effect of changing the solvent from H_2O to D_2O on the kinetics of the (pH-dependent; Fig. 3b) current fluctuations caused by the engineering of a glutamate at the pore-lining position 13′, in the middle of M2. We found that the high $\rightarrow$ low conductance-level transition is slowed down by a factor of ~1.5 ± 0.1, whereas the low $\rightarrow$ high transition is slowed down by a factor of ~3.2 ± 0.1 (Supplementary Fig. 4a). Interpreting these rates as proton-(deuteron-) association and dissociation rates, it follows that the pK_a of the introduced glutamate is upshifted by ~0.35 units (from 7.88 ± 0.01 in H_2O to 8.23 ± 0.02 in D_2O), a pK_a increase that is well within the range of values typically observed for free carboxylic acids in solution upon $H_2O \rightarrow D_2O$ solvent substitution [23–26]. On the other hand, in the case of the current fluctuations observed for the QQQEE mutant, we found that the forward and reverse rates change little upon changing the solvent and, possibly, both become faster –not slower– in the presence of D_2O on both sides of the membrane (Supplementary Fig. 4b). It seems safe to conclude, then, that the current fluctuations shown in Figure 2 do not result from the alternate association and dissociation of protons to and from the glutamates in the intermediate ring (or any other ionizable group in the protein), but rather, from a different phenomenon altogether.

A role for torsional flexibility in cation conduction

Position –1′ occurs at the most intracellular turn of the M2 α-helix[27–29]. With this in mind, examination of the different staggered conformations (or “rotamers”) that the glutamate side chain can adopt (Supplementary Fig. 5) suggests that some of these conformers would place the carboxylic/carboxylate moiety in the interior of the channel (collectively referred, here, to as “up” conformations), whereas others would orient these atoms away from the pore and toward the intracellular bulk water (“down” conformations). Considering the different extents to which the electrostatic effect of a negative charge is expected to be screened by these two microenvironments (a difference that, at least in part, arises from the slower reorientational dynamics of water in the confining structure of the transmembrane pore[30,31]),

it is reasonable to expect that a negatively charged carboxylate will affect the rate of cation conduction more when its Oε1/Oε2 atoms are “up” than when they are “down”. Thus, we hypothesized that the open-channel current fluctuations recorded from mutants of the XQXEE type (where “X” denotes any non-ionizable side chain; Fig. 2b) may well result from the conformational dynamics of the side chains of the two –1′ glutamates in the β1 and δ subunits. In the ~140-pS conductance level (Fig. 2c), both glutamates would position their carboxylates “up”, into the channel, where their effect on current amplitude would be higher. In the ~80-pS level, on the other hand, one of the carboxylates would be “up” and the other one would be “down”, the latter making a negligible contribution to the cation-conduction rate. Now, how about the wild type? In the context of this hypothesis, the notion that only two of the four glutamates of the wild-type AChR contribute to the size of the unitary current could be explained by proposing that, in a ring of four glutamates and one glutamine, two of the carboxylates are “up” and the other two are “down”. As for the protonation state of these side chains, their particular location squarely at the entrance of the pore (where water may still retain some bulk-like character) seems to ensure that all four carboxylates remain fully deprotonated even at pH 6.0 (Fig. 1b and Supplementary Fig. 6). Furthermore, the absence in the wild-type receptor of fluctuations between open-channel current levels of the sort observed for the XQXEE mutants could be the result of the “two-up–two-down” configuration simply being much more stable than any of the other competing configurations.

The torsional free-energy profile of an ionized side chain is expected to be sensitive to the local electrostatics. Indeed, one can predict that the probability of the –1′ glutamates occupying a “down” conformation decreases as the number of negative charges in the (intracellular) M1–M2 linkers increases. To test this prediction, we recorded single-channel currents from AChRs with a QQQEE intermediate ring and a variable number of acidic side chains at positions –5′ and –4′, and estimated the relative occupancies of the two open-channel current levels. Gratifyingly, the prediction above was borne out by the experiments: we found that, in going from a channel with M1–M2 linkers having no acidic side chains to one with four, six or seven aspartates (counting all five subunits), the ratio of low-conductance to high-conductance level occupancies decreases monotonically (Fig. 4a) as if the negative charges added to the intracellular side of the channel “pushed” the negatively charged Oε1/Oε2 atoms of the intermediate ring into the pore. Reassuringly, if the open-channel current fluctuations were due to protonation–deprotonation events, the relative occupancies of the conductance levels would be expected to vary in exactly the opposite way because the negative charges in the linkers would increase the proton affinity of the –1′ glutamates, and thus, would favor the low-conductance level. We also tested the effect of the membrane potential. Consistent with the proposed relationship between local electrostatics, glutamate side-chain conformation and single-channel conductance, hyperpolarizing the membrane (that is, making the cell’s interior more negative) favors the high-conductance level (Fig. 4b), much like adding aspartates to the M1–M2 linkers does.

Effect of location of the glutamates along the pore’s axis

Central to the hypothesis discussed above is the location of the glutamates in a region of the M2 segment that seems to provide a microenvironment of ambivalent properties. Certainly,

the glutamate's Oε1/Oε2 atoms would be positioned inside or outside the pore depending on the particular conformation adopted by the side chain. To test the plausibility of these ideas, we mutated the AChR as if to "slide" the intermediate ring of glutamates by one α-helical turn away from the cytoplasm, toward the pore's interior (Fig. 5a, b): we mutated the ring at position –1′ to a full ring of alanines and introduced glutamates at the pore-lining position 2′ in a variable number of subunits. Single-channel currents recorded from the construct bearing two glutamates at position 2′ (in the β1 and δ subunits, and with the corresponding wild-type residues in α1 and ε) revealed pH-dependent fluctuations of the open-channel current in the 6.0–9.0 pH range (Fig. 5c), consistent with the protonation–deprotonation of the engineered glutamates (interestingly, each glutamate engineered at position 2′ increases the conductance by ~50 pS, the same amount as each glutamate at position –1′ does when adopting an "up" conformation). It is likely that, in going from position –1′ to 2′, the properties of the aqueous microenvironment change in such a way that multiple negatively charged glutamates in close proximity can no longer avoid increasing each other's pK_a from the bulk value of ~4.4 into the 6.0–9.0 range. Notably, the response of this construct's open-channel current to pH resembles that of Ca_V and CNG channels, and thus, it demonstrates that a seemingly small structural change can turn a proton-insensitive channel, such as the wild-type AChR, into a proton-sensitive one. The addition of a third glutamate to the ring of residues at position 2′ confirms the finding about pH sensitivity noted above (Fig. 5d) and provides support for the hypothesis that the ability of glutamates to alternately "expose" and "hide" the negative charges to and from the pore depends tightly on their location along the α-helix. Indeed, when three glutamates are engineered at position 2′, every one of them adds a ~50-pS step to the "baseline" value of ~30 pS (for a total of ~180 pS). Similarly, in the case of the construct having four glutamates at position 2′, the conductance of the largest current level is ~230 pS (230 = 4×50 + 30), and discrete steps corresponding to the protonation–deprotonation of several binding sites are apparent (Fig. 5e). It seems as though glutamates at position 2′ cannot escape contributing to the size of the single-channel current; irrespective of the conformation of the side chain, the carboxylate moiety would always be inside the pore (compare Fig. 5a, b).

Subunit-specific side chain contribution to conduction

To gain insight into the symmetric-*versus*-asymmetric organization of side chains in the intermediate ring, we mutated the muscle receptor as if to rotate the wild-type side chains among the different subunits, positioning the single glutamine in β1 (EEEQE) or δ (EEEEQ). This procedure generated two mutants that, like the wild type, contain four glutamates and one glutamine at position –1′. Unlike the wild type, however, the EEEEQ mutant displays short-lived sojourns in a "super-conductance" level, consistent with the four glutamates briefly adopting a "three-up–one-down" configuration, whereas the EEEQE channel shows an increased open-channel noise that may well be the result of fast, ill-resolved open-channel current fluctuations (Supplementary Fig. 7a). These findings indicate that the side chains of the intermediate ring contribute to cation conduction in a subunit-specific manner; the positions of the side chains around the ring cannot be interchanged. We also engineered glutamines at position –1′ of the α1 subunits, thus giving rise to a ring with three glutamates (in β1, δ and ε) and two glutamines (in both α1 subunits). We found that the conductance behavior of this construct (QEQEE) resembles that of the receptor with a

single glutamine in δ (EEEEQ) in that the open-channel current fluctuates between a main level of ~135 pS and a superlevel of ~180 pS (Supplementary Fig. 7a); the relative occupancies of super- and main levels, however, are quite different in these two mutants. Moreover, the QEQEE receptor provides additional support for the notion that the AChR's single-channel current amplitude is not determined, simply, by the total number of glutamates in the ring. Certainly, with four such glutamates, the wild-type channel has a conductance that is lower than that of the QEQEE AChR's superlevel.

As shown in Figure 2a, channels having an intermediate ring of two glutamates in the β1 and δ subunits and three alanines (AAAEE) display a wild-type-like conductance. This observation led us to ask whether AChRs having any combination of two glutamates and three alanines at this position behave in the same way. As illustrated in Supplementary Figure 7b, we found this not to be the case. For example, when the two glutamates are present in the α1 subunits (EAEAA), the open-channel current alternates between two levels of conductance differing by ~40–50 pS (like other combinations of side chains shown here), but when the two glutamates are present in the β1 and ε subunits (AEAEA), the open-channel current consists, again, of a single level of wild-type-like conductance. These results reinforce the idea that each subunit of the muscle AChR makes a unique contribution to the functional properties of the intermediate ring and that whether the subunits carrying the two glutamates are adjacent or not (Supplementary Fig. 1b), for example, has no bearing on the observed behavior. Notably, all possible combinations of one glutamate and four alanines give rise to the same single ~80-pS level of open-channel current (Fig. 1a). We conclude, then, that it is the interactions between acidic side chains that are highly subunit specific. Furthermore, we conclude that the conductance behavior imparted to the AChR by any given combination of two or more acidic side chains cannot be easily predicted from the behavior of channels with other arrangements of the same number of acidic side chains around the intermediate ring, let alone from the behavior of channels with rings containing single such side chains.

Aspartates behave essentially like glutamates

Although all (known) AChRs from vertebrates contain four or five glutamates in the intermediate ring of acidic residues, several genomes from invertebrates and bacteria predict the existence of nicotinic-receptor-like channels containing aspartates, instead, at this position. Recordings from mutant muscle AChRs bearing different combinations of aspartates, glutamates, alanines and glutamines at position –1′ revealed that aspartate behaves, essentially, in the same way as glutamate (Supplementary Fig. 8). This includes the occurrence of fluctuations between two discrete levels of open-channel current in constructs of the XQXDD type. However, a closer inspection of some of the side-chain combinations revealed some intriguing differences. For example, when aspartates, glutamates and a glutamine were combined so as to give rise to the DQDEE AChR, the resulting open-channel current dwelled mostly in a wild type-like level (~154 pS), but short-lived sojourns in a level of higher conductance (~182 pS) could clearly be observed. This finding suggests that, in this mutant, although the "two-up–two-down" configuration of acidic side chains is still the most favorable one, occasional excursions to the "three-up–one-down" configuration cannot be avoided. Also, when the aspartates and glutamates of this construct

were swapped (thus generating the EQEDD AChR), the open-channel current seemed to consist of a single level of wild-type-like conductance (~143 pS), but the excess open-channel noise that is evident from the traces suggest that brief departures from the "two-up–two-down" configuration in either direction still occur. The much lower open-channel noise of the wild-type current indicates that the EQEEE combination of side chains is very effective at minimizing deviations from the "two-up–two-down" configuration.

DISCUSSION

Not much is known about the detailed structure of the intermediate ring of glutamates in the open-channel conformation of muscle-type AChRs. However, owing to their higher resolution, it is likely that the structural models of bacterial nicotinic-receptor-like channels can provide valuable clues and, in this respect, the model of the homomeric GLIC channel (although having the glutamates at position –2′ rather than –1′) seems to be the best approximation. Two models of GLIC at pH ~4 have become available, and one of the most prominent differences between them is, precisely, the conformation adopted by the glutamates of the intermediate ring. In one of the models (pdb code: 3EAM; ref. 28), all five glutamates position the carboxylate groups on the intracellular side, whereas in the other model (pdb code: 3EHZ; ref. 29), all five carboxylates are located in the interior of the pore (Supplementary Fig. 9). Although we would not necessarily take either model as an indication of what these glutamate side chains look like in the membrane-embedded channel (indeed, our results suggest that, in the AChR mutant having a ring of five glutamates, three of these would point "up" and two would point "down"), it is remarkable that the different crystallization conditions stabilized these side chains in two alternate conformations that are consistent with what our electrophysiological findings propose. Thus, the properties of the glutamate side chains described here for the muscle AChR may well represent a general feature of the intermediate ring of acidic side chains of all cation-selective members of the superfamily of nicotinic receptors. In Supplementary Figures 10 and 11, and Supplementary Table 1, we compare the structural models of rings of acidic side chains in the selectivity-filter regions of pentameric and tetrameric channels.

At this point, it may well be asked why previous mutational studies of the AChR's intermediate ring of glutamates failed to reveal the rich complexity that the data presented in this article has unveiled. We can only guess, but we surmise that the answer has to do, at least to some extent, with the duration of the recorded bursts of single-channel openings. Certainly, in the absence of burst-prolonging mutations engineered in the background, bursts of single-channel openings from many of the mutants studied here are as brief as (if not briefer than) the wild-type's, and hence, they are much too short for the fluctuations between discrete open-channel current levels to be fully appreciated and characterized (Supplementary Fig. 12). In retrospect, the fact that the fluctuations of the open-channel currents of the QQQEE AChR (in a wild-type background) went unnoticed in the seminal work of ref. 1 is not surprising.

The properties of the AChR's intermediate ring of glutamates differ in fundamental ways from those of the rings of acidic side chains in the selectivity filter of tetrameric-type channels. Most unexpectedly, whereas all four side-chains of the latter have been proposed

to contribute to set the size of the single-channel current[5–7], only two do so in the muscle AChR. It seems unlikely that the different number of amino-acid side chains in the ring (five *versus* four) has anything to do with this phenomenon. Rather, we favor the notion that it is the location of the ring along the long axis of the pore that plays a critical role. On the basis of our results, we put forward a mechanism in which the conformation of the acidic side chains in the unique microenvironment afforded by the transmembrane-pore–cytoplasm interface becomes a key determinant of cation-conduction properties. Admittedly, perhaps other ways of referring to the alternate states of the acidic side chains, such as “closer” and “farther”, “exposed” and “hidden”, “lumen-facing” and “non lumen-facing”, or “unshielded” and “shielded”, for example, provide a more accurate description of the mechanism underlying the observed phenomenon than the “up” and “down” labels used here. In the absence of conclusive structural evidence, though, we chose the latter largely for the sake of simplicity. Identification of the particular side-chain conformations underlying the proposed “up” and “down” states of the glutamates, elucidation of the physicochemical basis for the unique effect of glutamine (and, to a lesser extent, of asparagine) on the conformational free-energy profile of nearby acidic side chains, and clues into the evolutionary advantage conferred by a pore that eliminates pH sensitivity and minimizes open-channel noise will be the goal of future work.

METHODS

Currents were recorded from HEK-293 cells transiently transfected with complementary DNAs (cDNAs) coding the adult muscle-type AChR (mouse α1, β1, δ and ε subunits) or the α1 glycine receptor (GlyR; human or rat isoform b). Point mutations were engineered using the QuikChange site-directed mutagenesis kit (Stratagene) and were confirmed by dideoxy sequencing. Single-channel currents were recorded at ~22 °C from cell-attached patches with the exception of recordings that required access to both sides of the membrane, in which case the outside-out configuration with a constant application of ligand to the extracellular aspect of the patch was used. Ensemble (“macroscopic”) currents were recorded at ~22 °C from outside-out patches exposed to step changes in the concentration of ligand (solution-exchange $time_{10–90\%}$<150 μs; Supplementary Fig. 2b) as described in Supplementary Methods and ref. 32. The composition of all solutions used for electrophysiological recordings is indicated in Supplementary Table 2. pH values were measured with a glass electrode, whereas pD values were calculated by adding 0.40 units to the readings obtained with the same glass electrode used to measure pH values[26,33]; for both type of readings, the electrode was standardized with conventional H_2O buffers. Single-channel currents were digitized at 100 kHz, filtered (cascaded $f_c \approx$ 23 kHz) and idealized (using the SKM algorithm in QuB software; ref. 34) to obtain the corresponding dwell-time series and the current amplitudes of the different conductance levels. Dwell-time series were fitted with kinetic models (Supplementary Fig. 13; MIL algorithm in QuB software; ref. 35), using a retrospectively imposed time resolution of 25 μs, to estimate the rates of interconversion between the different levels of open-channel current. Current amplitudes were used to generate single-channel *i*–*V* curves. For all plots, error bars represent standard errors.

Supplementary Material

Refer to Web version on PubMed Central for supplementary material.

Acknowledgments

We thank S. Sine for wild-type muscle AChR cDNA; and A. Holmstrom, M. Pasquini, J. Pizarek and M. Rigby for technical assistance. This work was supported by a grant from the US National Institutes of Health (R01-NS042169 to C.G.).

References

1. Imoto K, et al. Rings of negatively charged amino acids determine the acetylcholine receptor channel conductance. Nature. 1988; 335:645–648. [PubMed: 2459620]
2. Galzi JL, et al. Mutations in the ion channel domain of a neuronal nicotinic receptor convert ion selectivity from cationic to anionic. Nature. 1992; 359:500–505. [PubMed: 1383829]
3. Bertrand D, Galzi JL, Devillers-Thiéry A, Bertrand S, Changeux JP. Mutations at two distinct sites within the channel domain M2 alter calcium permeability of neuronal $\alpha 7$ nicotinic receptor. Proc Natl Acad Sci USA. 1993; 90:6971–6975. [PubMed: 7688468]
4. Corringer PJ, et al. Mutational analysis of the charge selectivity filter of the α7 nicotinic acetylcholine receptor. Neuron. 1999; 22:831–843. [PubMed: 10230802]
5. Prod'hom B, Pietrobon D, Hess P. Direct measurement of proton transfer rates to a group controlling the dihydropyridine-sensitive Ca^{2+} channel. Nature. 1987; 329:243–246. [PubMed: 2442620]
6. Root MJ, MacKinnon R. Two identical noninteracting sites in an ion channel revealed by proton transfer. Science. 1994; 265:1852–1856. [PubMed: 7522344]
7. Chen XH, Bezprozvanny I, Tsien RW. Molecular basis of proton block of L-type Ca^{2+} channels. J Gen Physiol. 1996; 108:363–374. [PubMed: 8923262]
8. Hess P, Lansman JB, Tsien RW. Calcium channel selectivity for divalent and monovalent cations. Voltage and concentration dependence of single channel current in ventricular heart cells. J Gen Physiol. 1986; 88:293–319. [PubMed: 2428919]
9. Elenes S, Decker M, Cymes GD, Grosman C. Decremental response to high-frequency trains of acetylcholine pulses but unaltered fractional Ca^{2+} currents in a panel of 'slow-channel syndrome' nicotinic-receptor mutants. J Gen Physiol. 2009; 133:151–169. [PubMed: 19171769]
10. McDaniel DH, Brown HC. Hydrogen bonding as a factor in the ionization of dicarboxylic acids. Science. 1953; 118:370–374. [PubMed: 17813925]
11. Rajasekaran E, Jayaram B, Honig B. Electrostatic interactions in the aliphatic dicarboxylic acids: a computational route to the determination of pK_a shifts. J Am Chem Soc. 1994; 116:8238–8240.
12. Flocco MM, Mowbray SL. Strange bedfellows: interactions between acidic side chains in proteins. J Mol Biol. 1995; 254:96–105. [PubMed: 7473763]
13. Wohlfahrt G. Analysis of pH-dependent elements in proteins: geometry and properties of pairs of hydrogen-bonded carboxylic acid side-chains. Proteins. 2005; 58:396–406. [PubMed: 15558575]
14. Cymes GD, Ni Y, Grosman C. Probing ion-channel pores one proton at a time. Nature. 2005; 438:975–980. [PubMed: 16355215]
15. Cymes GD, Grosman C. Estimating the pK_a values of basic and acidic side chains in ion channels using electrophysiological recordings: A robust approach to an elusive problem. Proteins. 2011; 79:3485–3493. [PubMed: 21744391]
16. Bashford D, Gerwert K. Electrostatic calculations of the pK_a values of ionizable groups in bacteriorhodopsin. J Mol Biol. 1992; 224:473–486. [PubMed: 1313886]
17. Lancaster CR, Michel H, Honig B, Gunner MR. Calculated coupling of electron and proton transfer in the photosynthetic reaction center of *Rhodopseudomonas viridis*. Biophys J. 1996; 70:2469–2492. [PubMed: 8744288]

18. Qin J, Clore M, Gronenborn A. Ionization equilibria for side-chain carboxyl groups in oxidized and reduced human thioredoxin and in the complex with its target peptide from the transcription factor NFκB. Biochemistry. 1996; 35:7–13. [PubMed: 8555200]
19. Lindman S, Linse S, Mulder FA, André I. Electrostatic contributions to residue-specific protonation equilibria and proton binding capacitance for a small protein. Biochemistry. 2006; 45:13993–14002. [PubMed: 17115694]
20. Søndergaard CR, McIntosh LP, Pollastri G, Nielsen JE. Determination of electrostatic interaction energies and protonation state populations in enzyme active sites. J Mol Biol. 2008; 376:269–287. [PubMed: 18155242]
21. Bombarda E, Ullmann GM. pH-dependent pK_a values in proteins–A theoretical analysis of protonation energies with practical consequences for enzymatic reactions. J Phys Chem B. 2010; 114:1994–2003. [PubMed: 20088566]
22. Bell, RP. The Proton in Chemistry. 2. Cornell University Press; Ithaca: 1973.
23. Dahlgren G JR, Long FA. Relative hydrogen bonding of deuterium. I Ionization constants of maleic and fumaric acids and of their monoethyl esters in H_2O and D_2O. J Am Chem Soc. 1960; 82:1303–1308.
24. Glasoe PK, Eberson L. Deuterium isotope effect in the ionization of substituted succinic acids in water and in deuterium oxide. J Phys Chem. 1964; 68:1560–1562.
25. Glasoe PK, Hutchison JR. Deuterium isotope effect in the ionization of substituted malonic acids in water and in deuterium oxide. J Phys Chem. 1964; 68:1562–1563.
26. Salomaa P, Schaleger LL, Long FA. Solvent deuterium isotope effects on acid–base equilibria. J Am Chem Soc. 1964; 86:1–7.
27. Hilf RJ, Dutzler R. X-ray structure of a prokaryotic pentameric ligand-gated ion channel. Nature. 2008; 452:375–379. [PubMed: 18322461]
28. Bocquet N, et al. X-ray structure of a pentameric ligand-gated ion channel in an apparently open conformation. Nature. 2009; 457:111–114. [PubMed: 18987633]
29. Hilf RJ, Dutzler R. Structure of a potentially open state of a proton-activated pentameric ligand-gated ion channel. Nature. 2009; 457:115–118. [PubMed: 18987630]
30. Gutman M, Tsfadia Y, Masad A, Nachliel E. Quantitation of physical-chemical properties of the aqueous phase inside the phoE ionic channel. Biochim Biophys Acta. 1992; 1109:141–148. [PubMed: 1381612]
31. Fayer MD, Levinger NE. Analysis of water in confined geometries and at interfaces. Annu Rev Anal Chem. 2010; 3:89–107.
32. Elenes S, Ni Y, Cymes GD, Grosman C. Desensitization contributes to the synaptic response of gain-of-function mutants of the muscle nicotinic receptor. J Gen Physiol. 2006; 128:615–627. [PubMed: 17074980]
33. Glasoe PK, Long FA. Use of glass electrodes to measure acidities in deuterium oxide. J Phys Chem. 1960; 64:188–189.
34. Qin F. Restoration of single-channel currents using the segmental *k*-means method based on hidden Markov modeling. Biophys J. 2004; 86:1488–1501. [PubMed: 14990476]
35. Qin F, Auerbach A, Sachs F. Estimating single-channel kinetic parameters from idealized patch-clamp data containing missed events. Biophys J. 1996; 70:264–280. [PubMed: 8770203]
36. Ohno K, et al. Congenital myasthenic syndrome caused by prolonged acetylcholine receptor channel openings due to a mutation in the M2 domain of the epsilon subunit. Proc Natl Acad Sci USA. 1995; 92:758–762. [PubMed: 7531341]
37. Emsley P, Lohkamp B, Scott WG, Cowtan K. Features and development of *Coot*. Acta Crystallogr D Biol Crystallogr. 2010; 66:486–501. [PubMed: 20383002]
38. Humphrey W, Dalke A, Schulten K. VMD: visual molecular dynamics. J Mol Graph. 1996; 14:33–38. [PubMed: 8744570]
39. Lovell SC, Word JM, Richardson JS, Richardson DC. The penultimate rotamer library. Proteins. 2000; 40:389–408. [PubMed: 10861930]

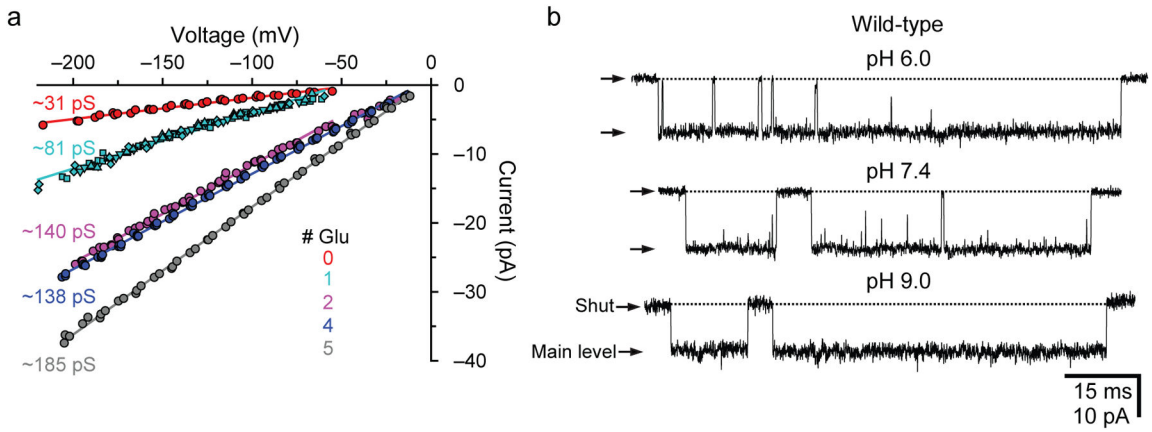

Figure 1. The intermediate ring of glutamates

a, Single-channel current–voltage (*i–V*) relationships (cell-attached configuration; 1 μM ACh; $pH_{pipette}$ 7.4) recorded from AChRs having zero, one, two, four, or five glutamates in the intermediate ring, as indicated in the text. Solution compositions are indicated in Supplementary Table 2 (solutions 1 and 2). To increase the mean duration of bursts of openings, the εT264P mutation[36] (at position 12′ of the M2 segment; Supplementary Figs. 1a and 2a) was also engineered. For the "one-glutamate" curve (▲, ■, ◆ and ▼), *i–V* data from all possible combinations of one glutamate and four alanines around the ring were recorded, and these are indicated with different symbols (one glutamate in either α1 subunit: ▲; one in β1: ■; one in δ: ◆; one in ε: ▼). For the data in this graph, whenever the ε subunit carried a (mutant) glutamate at position –1′, the "extra" glycine occupying position –2′ (or –3′; see Supplementary Fig. 1a) was deleted. **b,** Single-channel inward currents (outside-out configuration; 1μM ACh; solutions 3 and 4) recorded from the adult muscle AChR carrying the burst-prolongingεT264P mutation. The pH values of the extra- and intracellular solutions were the same. For the traces shown, the applied potential was −110 mV at pH 6.0, −100 mV at pH 7.4 and −80 mV at pH 9.0. Openings are downward deflections. Display f_c ≈ 6 kHz.

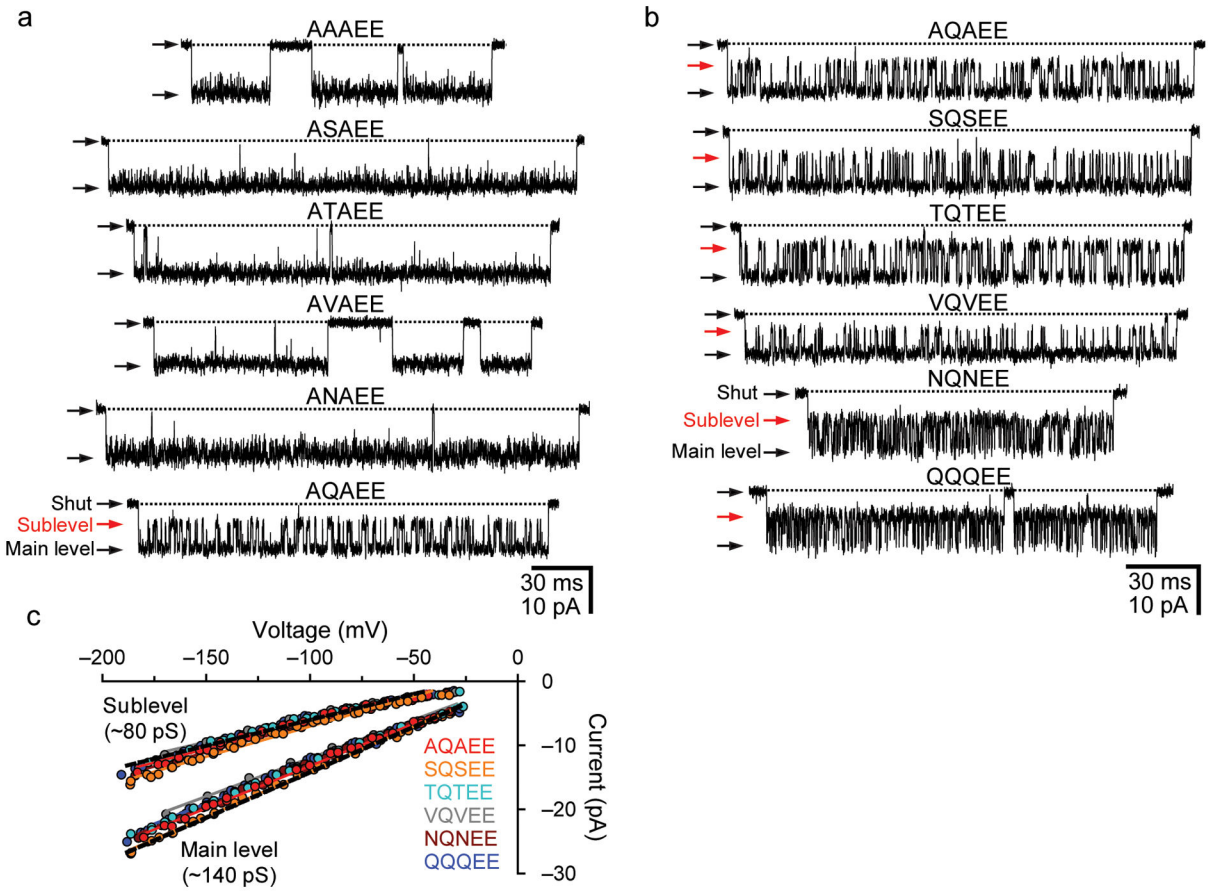

Figure 2. Mutations reveal a complex conductance behavior

a, b, Single-channel inward currents (cell-attached configuration; ~−100 mV; 1 μM ACh; $pH_{pipette}$ 7.4; solutions 1 and 2) recorded from AChR mutants containing different residues at position –1′; these are indicated using the single-letter code in the order: α1, ε, α1, β1 and δ subunits (see Supplementary Fig. 1b). All constructs also carried the εT264P mutation. We refer to the current level having a wild-type-like conductance as the “main level”. Openings are downward deflections. Display $f_c \approx 6$ kHz. **c,** Single-channel *i*–*V* curves recorded from the indicated six constructs under the same conditions as in **a** and **b**. The slopes of the main-level *i*–*V* curves are very similar to that of the two-glutamate AAAEE construct (~140 pS; superimposed black dashed line; see Fig. 1a), whereas the slopes of the sublevel *i*–*V* curves are very similar to that of AChRs bearing a single glutamate (the rest being alanines) in the intermediate ring (~80 pS; superimposed black dashed line; see Fig. 1a).

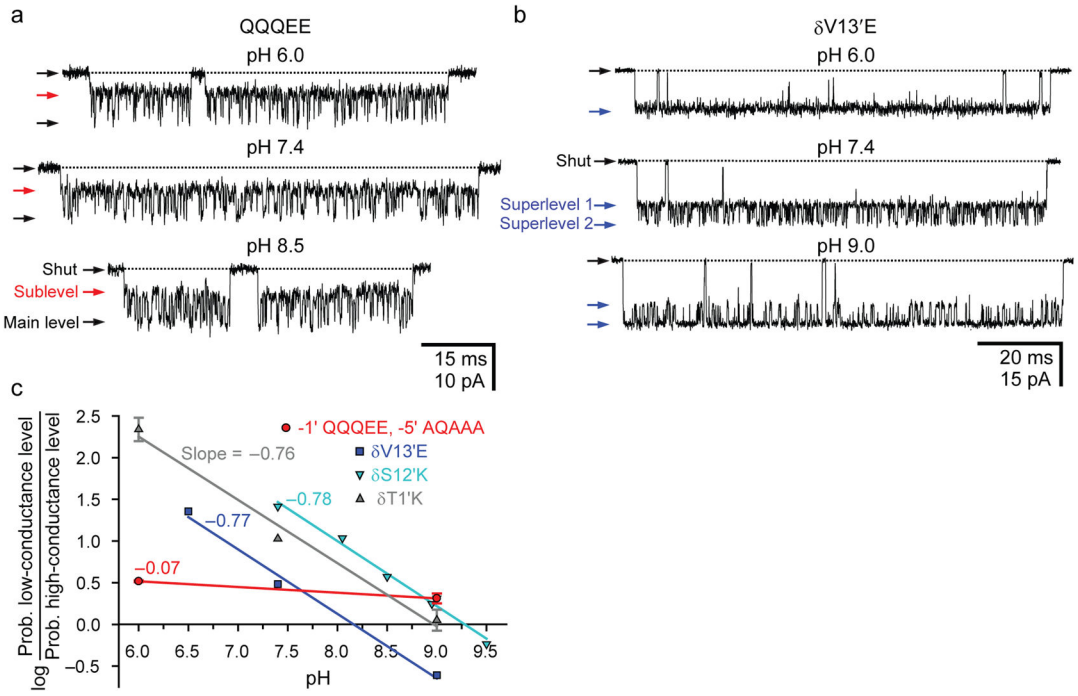

Figure 3. The pH dependence of intermediate-ring mutants is weak

a, Single-channel inward currents (outside-out configuration; −100 mV; 1 μM ACh; symmetrical pH; solutions 3 and 4). The construct also carried the εT264P mutation. **b,** Single-channel inward currents (cell-attached configuration; ~−100 mV; 1 μM ACh; solutions 1 and 2) recorded from the indicated mutant at position 13′ of the δ subunit. The indicated pH values are those of the pipette solution; for this mutant, bathing both sides of the membrane with solutions of the same pH was not necessary to reveal strong pH dependence. To increase the signal-to-noise ratio, the construct also carried two mutations in the ε subunit: a glutamine-to-glutamate mutation at position –1′ and the deletion of the "extra" glycine at position –2′. These ε-subunit mutations increase the single-channel conductance by ~50 pS ("superlevel 1"). The deprotonation of the glutamate engineered at δ13′ increases the conductance even further, by another step of ~50 pS ("superlevel 2"). For both, panels **a** and **b**, openings are downward deflections, and display $f_c \approx 6$ kHz. **c,** pH dependence of open-channel current fluctuations recorded from a mutant AChR containing the indicated residues at positions –5′ and –1′ in the background of the εT264P mutant (●; outside-out configuration; −150 mV; 1 μM ACh; symmetrical pH; solutions 3 and 5) and from the channel with a glutamate engineered at position δ13′ (■; cell-attached configuration; ~−100 mV; 1 μM ACh; solutions 1 and 2). Data corresponding to open-channel current fluctuations recorded from two δM2 lysine mutants (▼ and ▲; outside-out configuration; −100 mV; 1 μM ACh; symmetrical pH; solutions 3 and 5) are also included, for comparison.

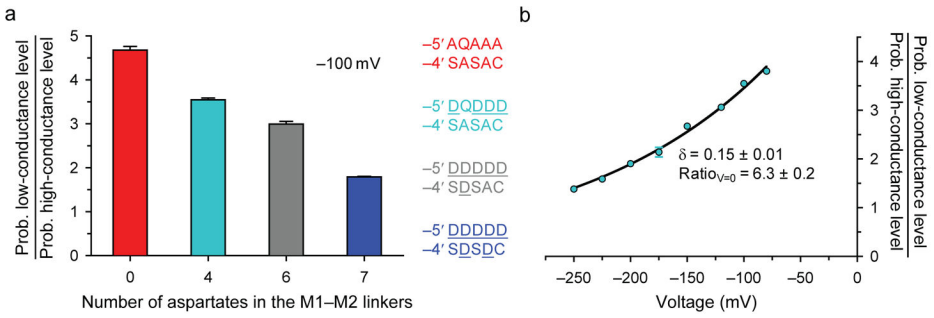

Figure 4. The conformational dynamics are sensitive to the local electrostatics

a, The effect of varying the number of aspartates at positions –5′ and –4′ of the M1–M2 linkers on the relative occupancies of the high and low open-channel conductance levels was estimated at ~−100 mV on AChRs having a mutant QQQEE intermediate ring (cell-attached configuration; 1 μM ACh; $pH_{pipette}$ 7.4; solutions 1 and 2). As is the case for position –1′, the residues occupying positions –5′ and –4′ are indicated using the single-letter code in the order: α1, ε, α1, β1 and δ subunits. Thus, the wild-type sequence is DQDDD at position –5′ and SASAC at position –4′. **b,** The effect of the membrane potential on the relative occupancies of the high and low open-channel conductance levels was estimated on the AChR having wild-type residues at positions –5′ and –4′, and a mutant QQQEE intermediate ring (cell-attached configuration; 1 μM ACh; $pH_{pipette}$ 7.4; solutions 1 and 2). The membrane potential ("voltage") is indicated as the potential on the intracellular side of the patch of membrane minus that on its extracellular side. The fit of the datapoints with a mono-exponential function [$Ratio = Ratio_{V=0}exp(\delta FV/RT)$, where V is the membrane potential, and F, R and T are Faraday's constant, the gas constant, and the absolute temperature, respectively] suggests that, at zero voltage, the plotted ratio of occupancy probabilities is ~6.3 and that the negative charge of the glutamate side chain traverses ~15% ($\delta = 0.15$) of the electric field upon switching between the "up" and "down" conformations. All constructs also carried the εT264P mutation.

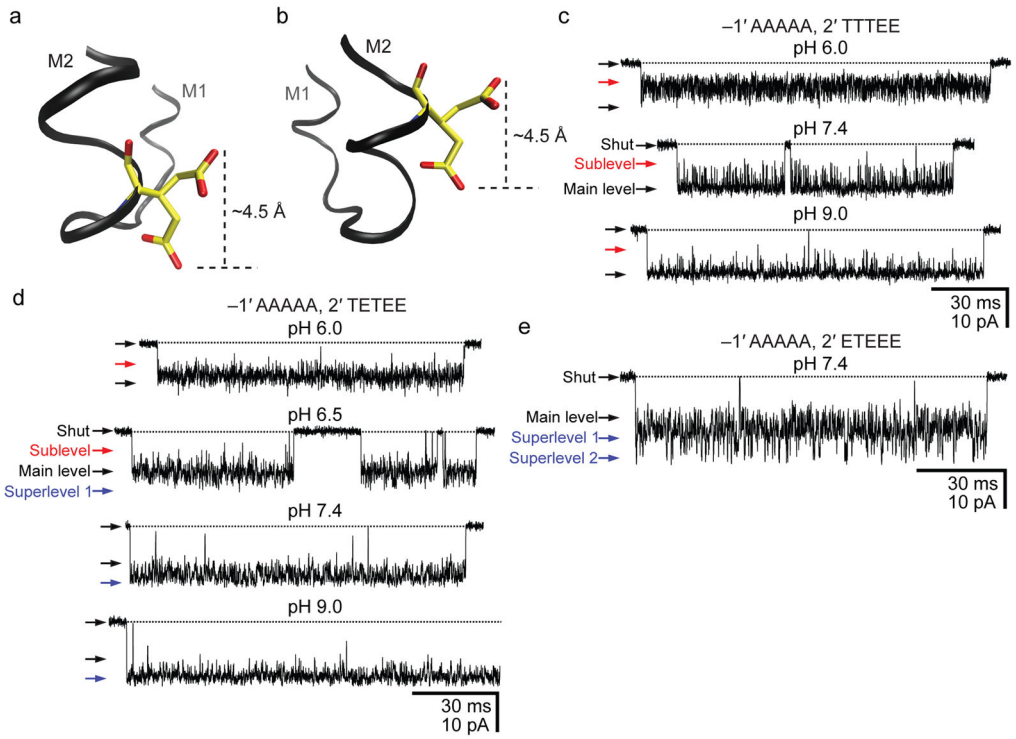

Figure 5. Moving the intermediate ring of glutamates into the pore

a, b, Two rotamers of glutamate. Using a model of the bacterial nicotinic-receptor-like GLIC channel (pdb code: 3EAM; ref. 28), a glutamate was "engineered" at position –1′ (**a**) or 2′ (**b**) using *Coot*[37] and VMD[38] molecular-graphics software (in GLIC, the wild-type glutamates of the intermediate ring occur at position –2′). The two conformers were chosen arbitrarily from the library of Lovell and coworkers[39] (see also Supplementary Fig. 5) and are merely meant to illustrate two extreme positions that the Oε1/Oε2 atoms could adopt. In going from position –1′ (**a**) to 2′ (**b**), it seems as though the glutamate would lose the ability to alternately "expose" and "hide" the negative charge to and from the pore; the charge would always be inside the pore. **c, d, e,** Single-channel inward currents (cell-attached configuration; ~−100 mV; 1 μM ACh; solutions 1 and 2) recorded from mutants containing the indicated residues at positions –1′ and 2′ (the latter, also in the order: α1, ε, α1, β1 and δ subunits). The indicated pH values are those of the pipette solution. The three constructs also carried theεT264P mutation. The current-amplitude scale is the same for all three panels. Openings are downward deflections. Display $f_c \approx 6$ kHz. We could not record currents from the mutant containing a full ring of alanines at position –1′ and a full ring of glutamates at position 2′ (~100 successful gigaohm seals with no channel activity).